

# VALIDATION OF CFD-BASED DATA SERVICE FOR DRONE INSPECTION OF WIND FARMS WITH FLIGHT TEST DATA

Keywords: drone, future flight, wind, urban airspace, wind farm, aerodynamics, CFD

*Mike Turner, James Sharpe, Max Kopacz, David Standingford - Zenotech Ltd*

*Carl Sequeira, Ben Sanby, Conrad Rider - Flare Bright Ltd*

## Abstract

The SnapShot drone was flown in the wake of the Bro Dyfi Community Renewables (BDCR) wind turbine in Wales and 5 flight traces were used to validate CFD modelling of the terrain and turbine. Comparisons were made between the flights and a RANS dataset based on a coarse mesh. After poor correlation was found due to the lack of historical weather data, mesh refinement revealed flow features were not being modelled correctly in the turbine wake. The resultant traces were investigated further using an Ensemble Fourier Transform (EFT) of unsteady simulations. Improved correlation was found when comparing the mean features of the frequency decompositions, but future work should focus on turbine model validation.

## Motivations

The global market for drones, advanced air mobility (AAM) and supporting services is circa \$74 billion by 2035 [UKRI, 2021] with the forecast market for services £4 billion. UKRI [UKRI, 2021] concludes that the case for change from the baseline services is sound in inspection, delivery, and sub-regional air-taxi. All operators need to manage risk, evaluate flight safety and have commercial requirements for insurance to fly. Meso-scale data suppliers include the UK Met Office that offers a UK Atmospheric Hi-Res Model with spatial resolution of approximately 2km with wind speed and direction at 10.0m height above ground level. This is well suited to the planning and execution of drone and other aircraft flights in open terrain, but it does not include the localised aerodynamic features (vortices and shear layers) that are required for the safe operation of aircraft. While more localised models can be produced, as with any simulation-based dataset, the method and model must be validated using independent data sources. Validated wind modelling of urban, airport and wind farm sites is a crucial element in the new landscape of UAV operation and data systems - particularly to support the safe and automated routing of drone-based inspection systems.

The SafeZone project supported by the Innovate UK “Future Flight” programme [UKRI, 2021] is a partnership between Zenotech (specialist in large-scale high-fidelity computational fluid dynamics-based aerodynamic modelling, including the AIRSIGHT™ aerodynamic data service), Flare Bright (developer of the SnapShot [Flare Bright, 2021] autonomous nanodrone that accurately measures wind vectors), Cardiff Airport and Cranfield University. SnapShot can reach areas where anemometers cannot and is significantly cheaper and provides more accurate data than LIDAR [Standingford et al,

2022]. The SafeZone project has conducted a programme of live drone flight trials at the Bro Dyfi Community Renewables (BDCR) wind turbine in Wales, where modelled steady and unsteady CFD datasets were compared with data from the SnapShot wind measurement nanodrone at a number of different locations including in the wake of the turbine.

## Testing with SnapShot

SnapShot is a lightweight autonomous drone with a patent pending software based wind measurement capability that allows it to act as an anemometer with a low cost, minimalist, sensor suite. Because of its nano-scale form factor, SnapShot can be safely used near infrastructure and along flight paths that are a perfect complement to ground-based and static anemometer systems. The CFD model is validated by using the SnapShot wind measurement nanodrone from Flare Bright Ltd, shown in Figure 1 on its launcher. Several flights were undertaken during the week of 13th November 2023, with detailed flight state and anemometry data recorded. In addition to the SnapShot data Flare Bright deployed a 5m high frequency anemometer to allow the SnapShot data to be cross referenced. The 5m anemometer location can be seen in Figure 6. SnapShot is launched vertically, and thus collects information in ascent and descent along an approximately vertical trajectory. This information can also be compared directly to the CFD model, run in RANS and DDES modes to correlate the high levels of flow detail recorded by the drone.

The dataset collected from the BDCR region consisted of a number of valid flights with 5 of them within the wake region of the turbine whilst the weather conditions permitted turbine rotation. The control system was enabled for the descent phase of the flight which adversely affects the data, rendering the downward portion of the measurements invalid. In some of the cases this is seen to affect the upper portion of the ascent parabola toward the vertex. Additionally, higher frequency fluctuations above 20 metres were not measured, therefore only bulk flow features were captured in the turbine wake region.



*Figure 1: SnapShot autonomous nanodrone on its launcher, set-up downstream of the wind turbine prior to flight test*

## Modelling

To model the wind conditions experienced at and in the wake of the turbine, a RANS CFD simulation was performed over a  $25\text{km}^2$  domain centred at the wind turbine in question. Initially, the terrain model was based on the Terrain 5 Dataset available from Ordnance Survey, akin to the parameters published in previous work [Standingford et al, 2022], with the addition of a turbine performance and wake model based on operation data from BDCR. A  $25\text{km}^2$  square domain was divided into  $1000 \times 1000$   $5 \times 5\text{m}$  quads which were then plane mapped to the corresponding points given by the Terrain 5 dataset. This created a convex hull terrain surface mesh which was used to grow a volume mesh. Here the boundary layer was meshed with an initial first cell height of  $1\text{m}$  with a vertical expansion ratio of  $1.3$  and a global background mesh spacing of  $50\text{m}$ . The geometry was automatically refined in areas of high curvature and gradient and a refinement zone of radius  $750\text{m}$  around the turbine limited the minimum cell size to  $5\text{m}$  in this region in a  $75\text{m}$  radius from the terrain. Outward of this region was a decay radius of  $2000\text{m}$  where spacing was relaxed to a minimum of  $10\text{m}$  and automatic curvature and gradient control dominated the local refinement. The resulting terrain, due to decimation, had approximately 6 million cells. The wind turbine is modelled as an actuator disk (familiar to aerospace CFD practitioners) that captures the averaged power production, thrust and torque effects of a wind turbine. The turbine model itself uses blade element theory (BET) based on the turbine blade dimension, and the spanwise lift and drag coefficients as functions of Reynolds number, rate of rotation and local angle of attack (pitch). The mesh featured a structured butterfly topology containing approximately 528,000 cells given its length was  $4 \times$  the rotor diameter, whilst 54 cells span the actuator disk face. The disk face, as

processed by the solver is represented in Figure 2, whilst the overset case in the context of the BDCR terrain surface mesh is shown in Figure 3.

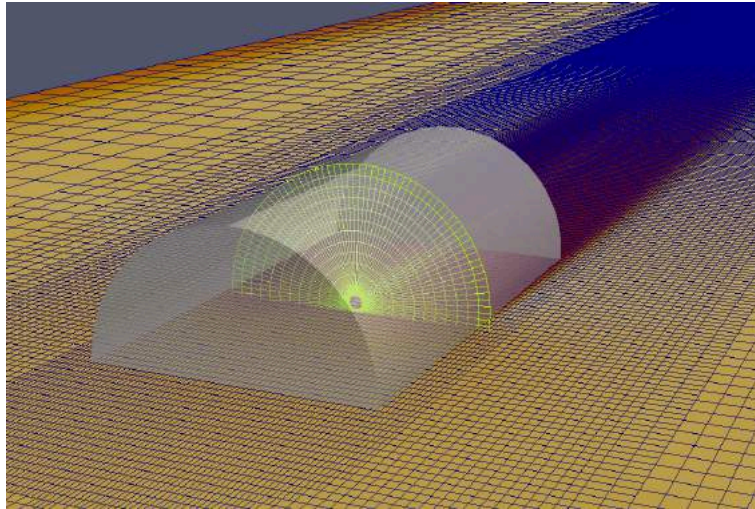


*Figure 2: Turbine model as an actuator disk based on Blade Element Theory. The actuator disk (yellow) is superpositioned on an existing CFD mesh, and used as the basis for thrust and torque momentum sources. The sources are derived from the lift and drag characteristics of the turbine blades, averaged over a complete rotation. Further information on the implementation is available [zCFD Reference Guide] following [Creech, 2009].*

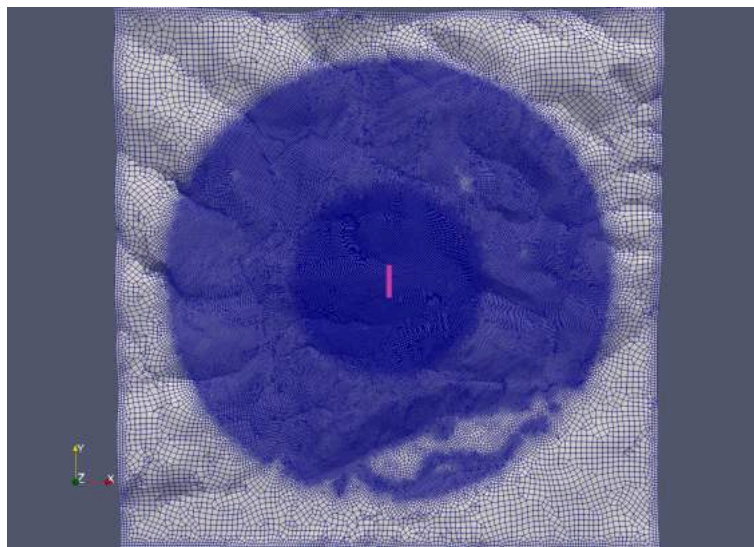


*Figure 3: Surface mesh of the BDCR terrain overset with the volume mesh of the turbine (pink) aligned to flow from the North (positive Y)*

Further solver parameters generally followed previous work regarding roughness length scales, which were remapped for the new domain. A noteworthy simplification in this model is the omissions of physical building models, as opposed to the standard practice when terrain modelling, due to the area of interest around the turbine being relatively remote and away from any buildings. The buildings are therefore simply modelled as having a roughness length of 1m. Otherwise, the solver parameters are identical with the exception of the multigrid level, which was pushed to 3 to improve convergence in flows above 4 m/s. Below this value, solver failure rate increased due



to the poor matrix conditioning experienced at these lower speeds; a switch was implemented which reduced the multigrid to 2 when below 4 m/s, allowing for an initial wind rose of simulations to be constructed. This is required for predicting turbine wake regardless of the weather conditions to avoid extrapolation. The wind rose shown in Figure 4 shows wind speeds ranging from 5-15 m/s as these covered the ranges of wind speeds explored during the snapshot test flights.

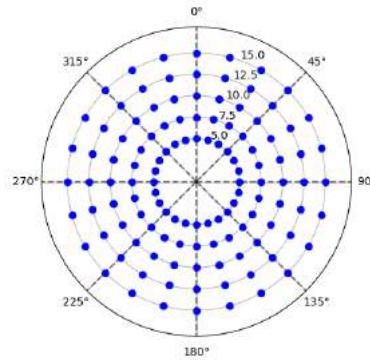


Figure 4: Complete wind rose illustrating the *cfD* initial conditions (blue) with inflow speeds represented by the concentric circles and inflow bearing as the radii

To establish solid correlation between the SnapShot results and the CFD model, a physically accurate inflow atmospheric boundary layer (ABL) was implemented. Due to the variation in modelled wind speed inside the area of interest relative to the inflow conditions, data comparison had to be performed by querying wind conditions at the time of each SnapShot launch. Historic meso-scale atmospheric data was not available for such a remote location and attempts made to correlate historical weather data [Skylink, 2024] taken from the closest weather station: Cardiff airport, were poor, as outlined in Figure 5.

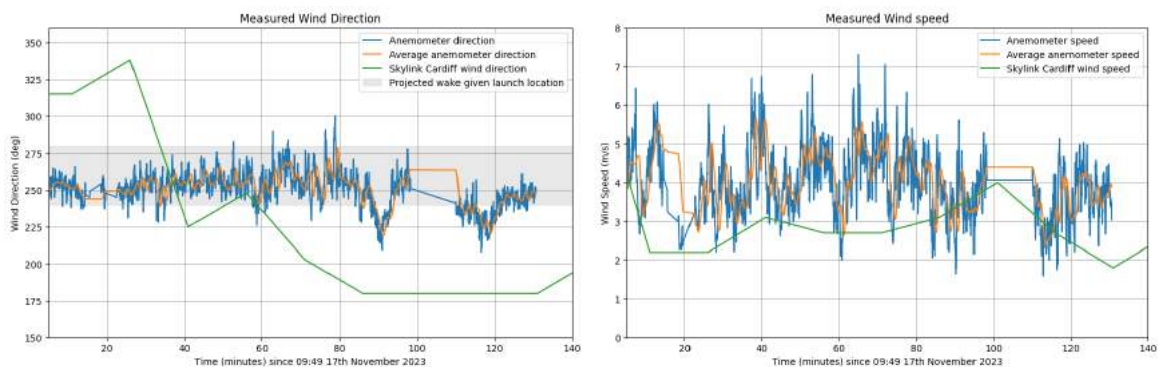
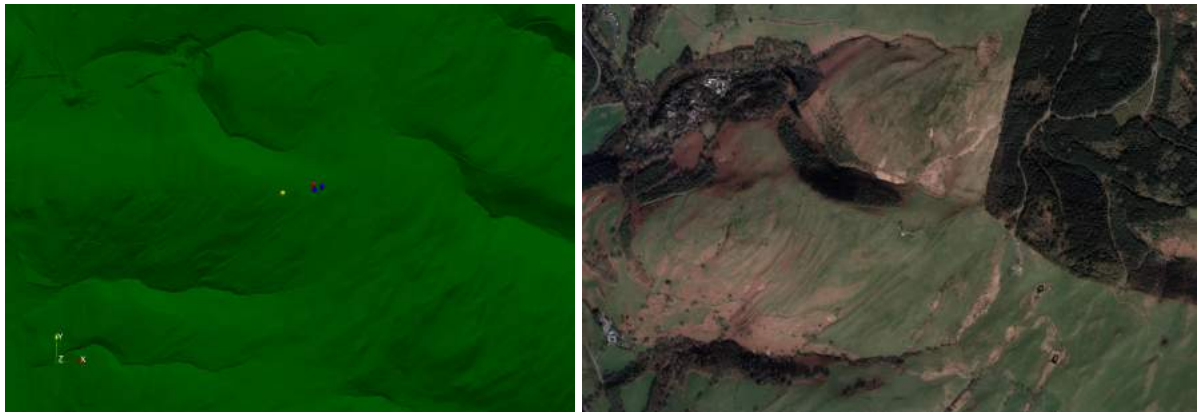


Figure 5: Comparison of anemometer angles and speeds with Cardiff skylink data with predicted wind directions given the flight locations and the turbine wake

To determine the most representative wind condition for each flight, three primary methods were used: 5m **anemometer** data averaged over the flight duration; an average of the first 20 metres of the snapshot launch (lower portion of flight not in turbine wake); and the 10 minute average turbine anemometer data. The use of all of these sources emphasises the difficulty in predicting the initial conditions for the solver, all with their limitations. The locations of these data sources are visualised on the

modelled surface in Figure 6.



*Figure 6: [Left] Turbine anemometer (yellow), 5m anemometer (red) and SnapShot launch (blue) locations overlaid on the BDCR terrain model (green) from a plan view. [right] BDCR satellite image [Google Earth, 2024]*

The initial conditions could then be reconstructed given a target wind speed at a height, reproducing the inflow ABL through modifying the corresponding friction velocity via the zCFD interface as outlined in the zutil module and details on the implementation can be found [zCFD Reference Guide] following [Zhang, 2009].

When considering the 5m anemometer, placed at a vertical height of 5m off the ground, the high frequency unsteady fluctuations close to the terrain exhibited a large sensitivity to the initial conditions. In addition, the 5m anemometer does not measure the z-velocity components due to its single axis of rotation, which are relevant so close to the hilly terrain. SnapShot mitigates this issue through using its wind measurement system to record all three velocity components. It is also subject to the unsteady fluctuations which are often good representations of the bulk flow at the time of launch. Therefore it was concluded that the ABL height was fixed at 30m, allowing runs to be completed throughout the wind rose. By setting the zCFD profile height, the desired flow speed was targeted at the turbine hub (anemometer) height. This profile is mapped to the terrain and treated as an initial boundary condition, however, as the flow travels over the 2.5km of modelled terrain before it reaches the actuator disk, the turbine experiences a resolved ABL based on the upwind terrain. Figure 7 outlines the effect of capturing the ABL using a cell growth factor away from the terrain (wall) surface.

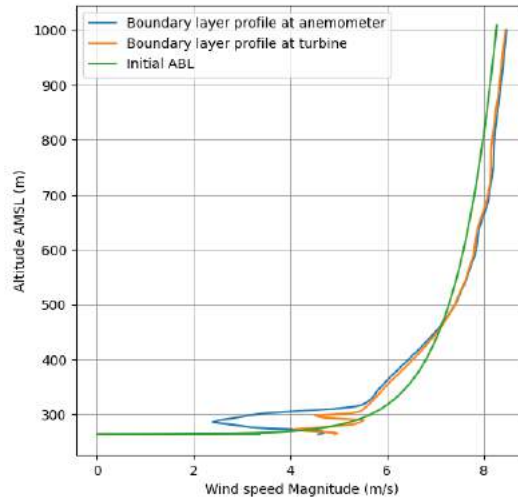


Figure 7: Inflow ABL compared against the ABL experienced at the turbine and the anemometers within the regions of interest in the turbine wake, which can be seen through the decreased velocities through 280-310 m as a result of the actuator disk

## Processing and correlating SnapShot data

Following the snapshot data correlation conducted in previous studies [Standingford et al, 2022], data collection was improved through representing the points as a polynomial line which the cfd volume data solution could be efficiently resampled to. The wind velocity profiles for each initial condition of the wind rose were extracted, along with the wind speed at the 5m anemometer and one turbine diameter upwind of the turbine hub. Performing this preprocessing step and storing them in dictionaries allowed for fast data mark up, and set up a framework for interpolation between runs. The recorded 5m anemometer, SnapShot average and turbine anemometer speeds were all used as query points for interpolation and they are represented in Table 1. The speeds extracted for each location showed the variation of wind speed through the ABL, as the wind speed increased with height. Additionally the unsteady nature of the flow is apparent through the variations in directions between measurements on the same flight, which were all taken at the same moment in time.

Table 1: Speeds and angles recorded by each data source for each flight number (#)

	#15 (m/s, °)	#17 (m/s, °)	#19 (m/s, °)	#26 (m/s, °)	#28 (m/s, °)
5m Anemometer	4.1, 251	4.4, 262	3.9, 253	4.4, 247	5.2, 269
SnapShot 20m Average	5.1, 255	5.5, 271	5.4, 260	7.2, 278	6.4, 271
Turbine Average	6.8, 264	7.2, 264	6.7, 264	7.1, 261	7.3, 261

By normalising the wind speeds and angles recorded at each of these monitor points in the CFD simulation, a grid of conditions was established. Through setting a cubic spline interpolation between the points, the resultant surrogate model is continuously

differentiable within its convex hull as seen in Figure 8.

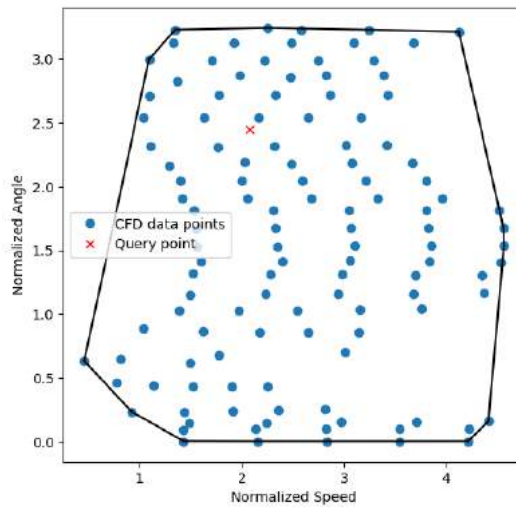


Figure 8: Convex hull representing the extent of the surrogate model containing flight trace data taken from the points around the wind rose and the corresponding wind speeds and directions at each location, shown is the 5m anemometer model for Flight 19

Therefore, for a given wind speed measurement, a trace could be efficiently reconstructed along the flight path of the SnapShot launch and the velocity magnitudes were directly compared for validation as showcased in Figure 9. This process is automated allowing for reproducible data given different meshes and wind rose specifications, lending to the versatility of SnapShot data collection and the vast range of environments drones will be operating in.

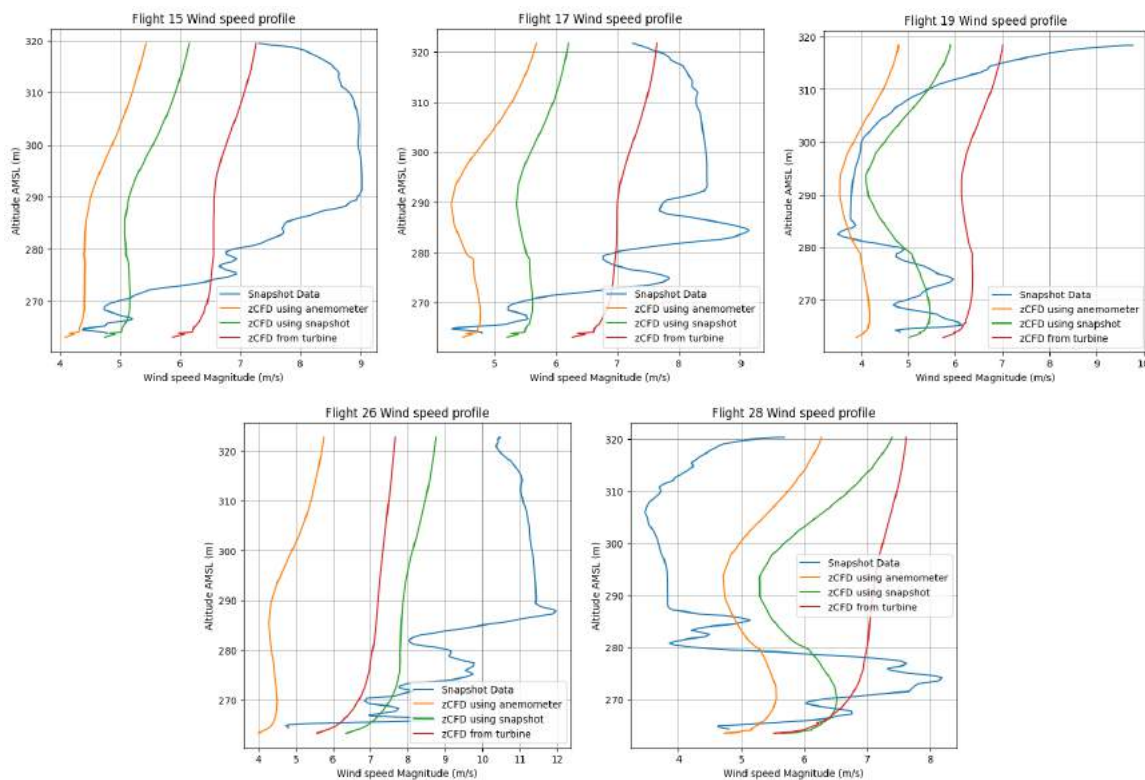




Figure 9: Velocity magnitude profile comparison of snapshot and CFD using three free stream query metrics and interpolating using closest angle and velocity

The results of correlating the data clearly show a high sensitivity with the velocity profiles to the query locations in the cfd data. In previous studies the use of weather data would avoid this by comparing atmospheric flow conditions to the 5m anemometer data. However, the complex interactions with the 5m anemometer and the terrain caused varying levels of accuracy between flights and this matrix. Similarly, as the angle implied by the turbine anemometer is estimated by the angle between the turbine and the launch locations as the launches occurred in the wake of the turbine, the actual angle would have varied with time. To capture this effect a wider spread of launch locations would be required.

SnapShot provides an instantaneous look at the wind conditions along its flight path. The flow features it experiences are subject to unsteady fluctuations as it traverses through turbulent flow regions. To confirm whether the models are correct and can successfully predict flow features measured by the probe drone it is imperative to explore the fidelity requirements as to reduce computational cost where possible whilst accurately predicting unsafe or potentially hazardous regions for aircraft to operate in. The launch locations in this case were well known, giving a narrower region of testing compared to the general case for a given environment. The effect of denser modelling within a more targeted wind rose are outlined in Figure 10.

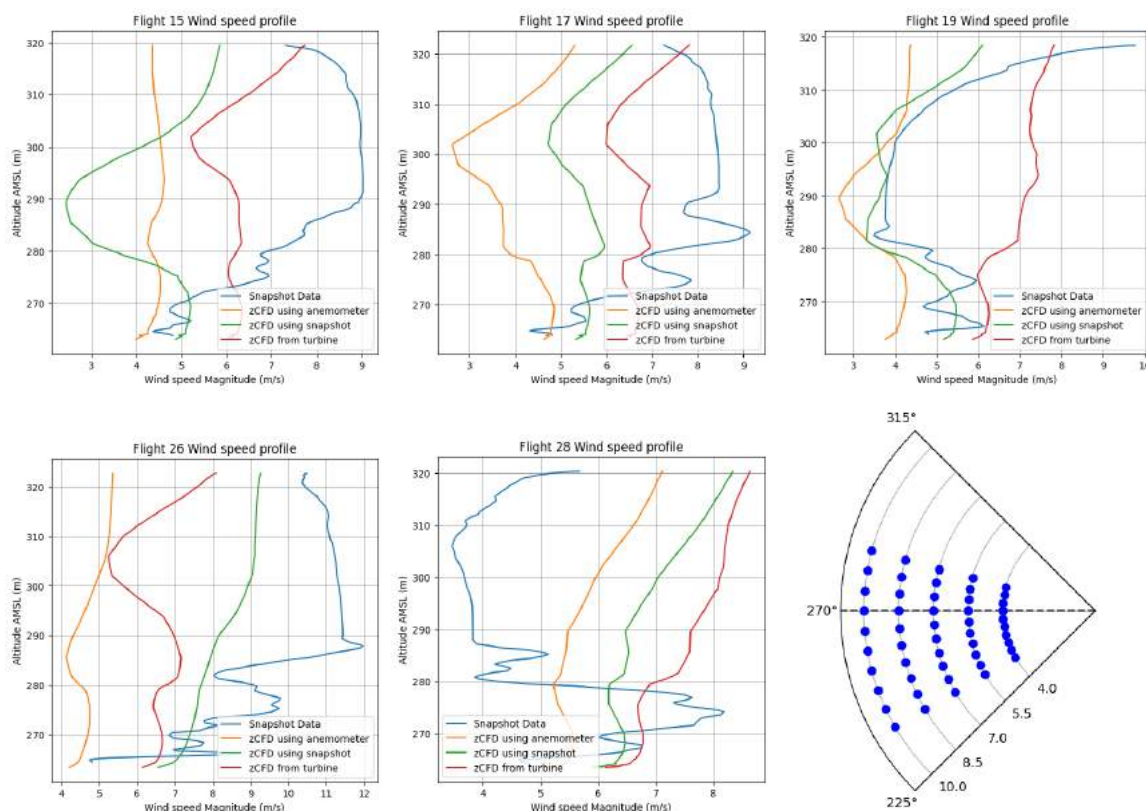


Figure 10: Velocity profiles given a narrower wind rose (bottom right) for every snapshot flight. 50 simulations were performed at 5 degree and 1.5 m/s intervals with flight 19

*showing the most promise. Little to no improvement in correlation was found in comparison to the whole wind rose*

Further investigation into fidelity requirements led to the construction of a higher resolution mesh. An apparent limitation of the coarser mesh was the inability to capture the fluctuations seen on the flight data. Additionally the jagged nature of the traces suggests poor solution reconstruction at this resolution; mesh refinement gave way to a 74.0 million cell mesh with 1m refinement centred in a 500m radius around the area of interest.

## Terrain Investigations

Whilst the 5m Ordnance Survey terrain model was generally sufficient, an investigation was conducted into a more accurate terrain model. The Welsh government offers 1m resolution Digital Terrain and Surface Models (DTM and DSM respectively) of the entire country available for download stored as LIDAR .tiff files [DataMap Wales, 2023]. Similar datasets are available for the rest of the UK, and can be considered for future cases. The much simpler digital terrain model was used for the refined surface as the roughness lengths mapped to the surface represented the physical features in the DSM dataset. The way the DTM was constructed was by mapping a 1m height contour onto a 1x1m grid. Therefore meshing attempts often failed due to the sudden steps in height due to the contours, additionally, the generated terrain was non-physical. To mitigate this and to allow for a representative terrain surface to be recovered, the contours were extracted and the points which lay on the contour lines were used to represent the gradient changes in the terrain as seen in Figure 11. The transition between contours was much smoother than the original dataset, and the Delaunay triangulation used to connect the points created a highly detailed terrain surface. Additional points were placed around the bounding box of the domain as the contours did not cover the whole extent, and to ensure a watertight mesh, the domain stl which the volume mesh grows from must cover the entire domain. These were taken from the original LIDAR domain and input to the triangulation routine. This method was highly computationally efficient and allowed for easy meshing of large areas as the process is highly parallelizable due to domain partitioning.

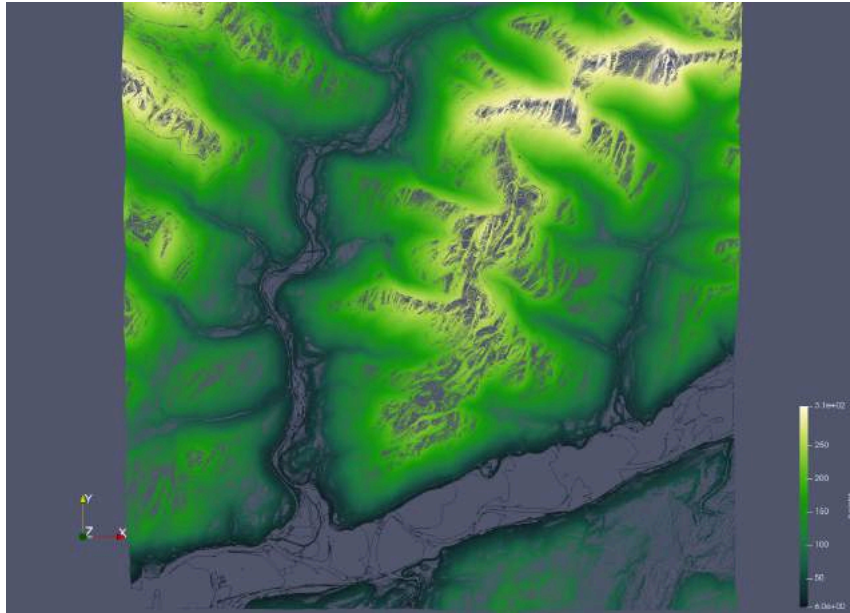


*Figure 11: 1m height contours of higher resolution DTM LIDAR data of the simulated BDCR domain, used as a basis for terrain surface meshing*

To reduce the cell count, a narrowed decay region of 800m around a 500m refined region from the turbine was selected, with a coarser global background spacing of 75m, allowing for a 72.6 million cell mesh. A comparison of mesh cross sections can be seen in Figure 12 where the difference in detail between the two models clearly shows additional features present in the 1m surface model.

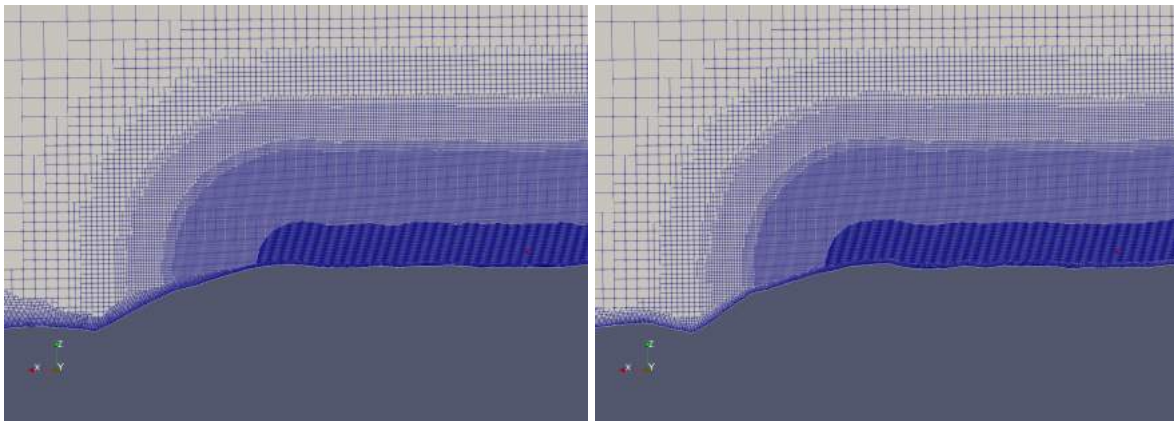


*Figure 12: Comparison of the 5m LIDAR surface refined mesh (left) and the 1m LIDAR surface refined mesh (right) with the turbine location marked in red looking from the North.*

To investigate the effect of the refined meshes on the flow, it was not prudent to conduct testing about the whole wind rose due to the increased computation and so a single design point was chosen based on the most closely correlated result found from the lower resolution runs. A least squares distance of the completed runs found the 255° case at 5.5 m/s produced the closest results to the flight profile captured in flight 19. Visually, this was the flight which showed the most promise as it was reasonable to assume the freestream flow variables were well aligned with the flight conditions at

the time of testing. This was therefore used as a basis to conduct further model testing, and the resulting profiles are shown in Figure 13.

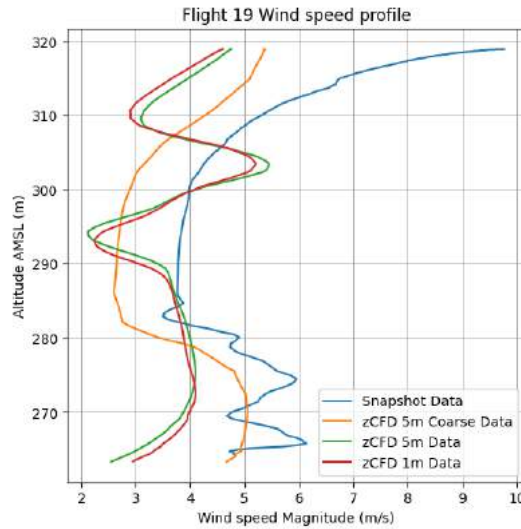


*Figure 13: Wind speed profiles for the three different meshes for the conditions experienced in SnapShot flight 19. There is little difference between the higher resolution solutions despite the change in terrain model, however it is clear that the actuator disk wake is much more prominent and the boundary layer is better resolved compared to the coarse dataset*

Whilst more features are recovered using a finer mesh, SnapShot provides an instantaneous measurement of the unsteady flow, therefore to correctly predict a safe region of operation around the turbine, the frequencies experienced in the wake can be used to quantify this.

## Unsteady Simulation

Akin to the investigations conducted by [Standingford et al, 2022], unsteady investigations of the SnapShot profiles provide a useful metric to determine correlation. For this case, due to the varying conditions between flights, only one flight could be compared against the cfd result as performing an unsteady run for each case was largely infeasible, therefore this study is a continuation from the higher resolution RANS cases for flight 19. A DDES hybrid unsteady simulation was run, simulating 50 seconds of real time, with a dual time stepping scheme completing 50 pseudo time steps to reach convergence, given an explicit time marching scheme, for each 0.1 second real time step. Similarly to the previous study, an Ensemble Fourier Transform (EFT) was performed for flight 19 and the corresponding trace was sampled over each unsteady timestep of the cfd simulations. The results in Figure 14 compare the averages found with the two higher resolution meshes, with a 1 standard deviation error bar. As this inflow condition was only valid for one flight, the EFT over SnapShot data could not be conducted over multiple flights.

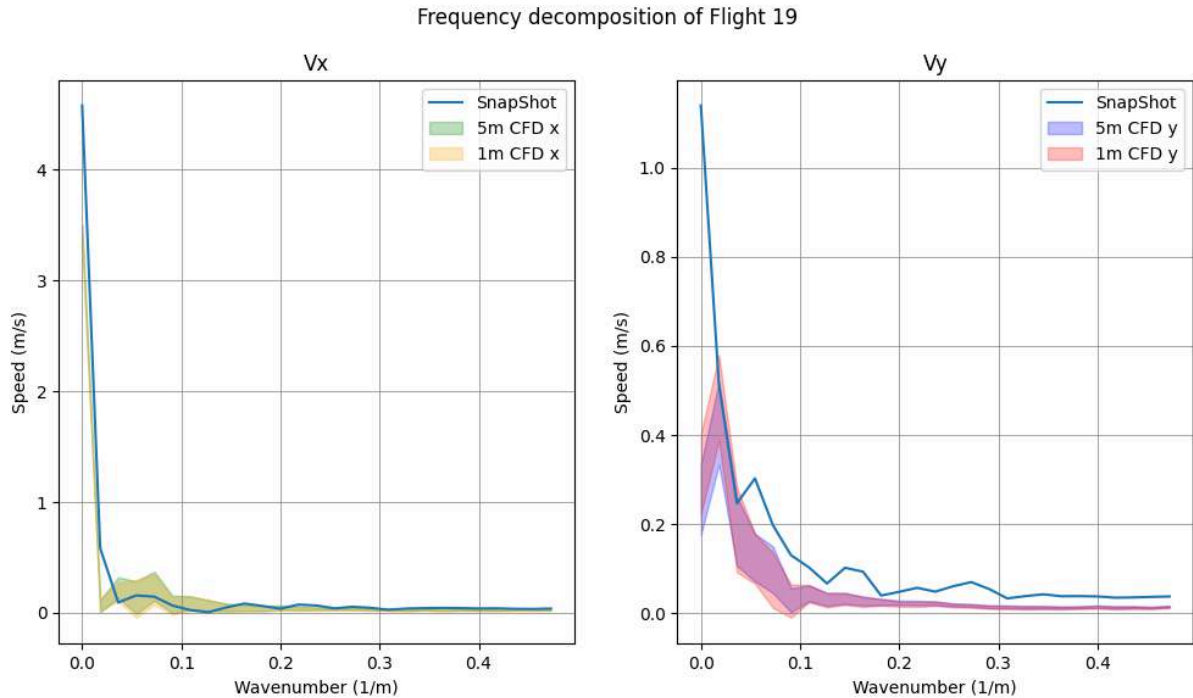


Figure 14: EFTs for SnapShot flight 19 and the unsteady CFD datasets for the two terrains. Generally the trends seem to be in agreement with little variation between the two terrain models. The y velocity,  $V_y$  has much greater standard deviations, and generally has poorer correlation with the measured data, which is exaggerated by the smaller velocities compared to the x component,  $V_x$

An additional feature of the EFT is greater uncertainty between wavenumbers 0.05-0.1. A feature of the actuator disk modelled used is the hole at the centre of the disk surface in place of the turbine hub. In the unsteady simulations this was seen to produce a Karman vortex street and could be a prominent feature of the frequency decomposition, further investigations would be required over larger datasets to quantify this.

## Conclusions and recommendations

SnapShot testing revealed unsteady velocity profiles within the wake of the BDCR turbine. As weather data was not available to correlate the 5m anemometer data with the atmospheric flow, three data sources were used to reconstruct a boundary condition for the CFD simulation. RANS on a coarse mesh was used to create a surrogate model using cubic splines for fast trace reconstruction for the given launch locations. This was refined through increasing the number of simulations, making the query points more representative of the CFD solution, but not improving correlation. The poor correlation inspired investigations into mesh refinement. Flow features not present in the lower resolution runs were simulated in the finer mesh, again not improving correlation. This was also true when refining the terrain topology. Only when comparing the unsteady datasets was a better correlation found, suggesting that due to the instantaneous nature of the SnapShot data collection, it is highly sensitive to the time variant fluctuations. These unsteady runs would also benefit from a higher fidelity turbine model as further work would need to be conducted to ensure the the



effects of the actuator disk model are representative of the conditions captured by SnapShot.

Future work would also consist of ensuring SnapShot traces were valid throughout the entire portion of the flight and producing more flight examples for different wind speeds and directions. A limitation of this approach was the launch location only testing model correlation for one section of the terrain. Given the complexity of the terrain, an increase in the amount of collected data is required to ensure that this methodology is robust.

## Contact author email address

The corresponding author is Mike Turner: [mike.turner@zenotech.com](mailto:mike.turner@zenotech.com)

## Acknowledgement

We gratefully acknowledge support from UKRI Innovate UK under the “Future Flight Challenge Phase 3” project number 10025740.

## Copyright statement

The authors confirm that they, and their company hold copyright on all the original material included in this paper. The authors also confirm that they have obtained permission, from the copyright holder of any third party material included in this paper, to publish it as part of their paper. The authors confirm that they give permission or have obtained permission from the copyright holder of this paper, for the publication and distribution of this paper as part of the ICAS proceedings or as individual off-prints from the proceedings.

## References

- [Appa et. al., 2021] “Performance of CPU and GPU HPC Architectures for off-design aircraft simulations.” AIAA 2021-0141, <https://doi.org/10.2514/6.2021-0141>
- [Creech, 2009] “A three-dimensional numerical model of a horizontal axis, energy extracting turbine: An implementation on a parallel computing system”, Angus C.W. Creech, Heriot-Watt University, Scotland, March 2009.
- [Flare Bright, 2021] SnapShot drone, UK Registered Design 6160829, <https://flarebright.com/>
- [Saeed, 2019] “Affordable Modelling of Complex Extreme Events in the Built Environment Using GPU-accelerated CFD”, NVIDIA GTC 2019, <https://developer.nvidia.com/gtc/2020/slides/s21373-affordable-modeling-of-complex-extreme-events-in-the-built-environment-using-gpu-accelerated-cfd.pdf>
- [Standingford, 2019] “Rapid RANS wake simulation with customisable turbine models: CPU / GPU with Python interface”, WindEurope Conference PO175.
- [Standingford et al, 2022] “Validating Airspace CFD Models For Drone Operation with Flight Test Data”. 33rd Congress of the International Council of the Aeronautical Sciences (ICAS2022), Stockholm, Sweden. (2022, November 28) <https://doi.org/10.5281/zenodo.7380689>
- [UKRI, 2021] “Future Flight Vision and Roadmap”, UK Research and Innovation report UKRI-130821, August 2021.

**[Google Earth, 2024]** Google Earth, 52.619093°N, 3.829728°W, 252 m, Bro Ddyfi Community Renewables, <https://earth.google.com/>

**[Wainwright et. al., 2021]** “High Fidelity Aero-Structural Simulation of Occluded Wind Turbine Blades”, AIAA20210950. <https://doi.org/10.2514/6.2021-0950>

**[DataMap Wales, 2023]** Welsh LiDAR Dataset, March 2023.

**[Zhang, 2009]** CFD simulation of neutral ABL flows. Danmarks Tekniske Universitet, Risø Nationallaboratoriet for Bæredygtig Energi.

**[Skylink, 2024]** Historical Weather Data. Available at: <https://skylink-pro.com/> (Accessed: 14 June 2024).

<https://datamap.gov.wales/maps/lidar-viewer/>

**[zCFD Reference Guide]** <https://zcf.dzenotech.com/>

**[zCFD User Guide]** <https://zcf.dzenotech.com/docs>

**[zCFD Validation Cases]** <https://zcf.dzenotech.com/validation>